Applied Thermal Engineering 116 (2017) 43–55

Contents lists available at ScienceDirect

Applied Thermal Engineering

journal homepage: www.elsevier.com/locate/apthermeng

Research Paper

Experimental research on convective heat transfer of supercritical hydrocarbon fuel flowing through U-turn tubes

Yanchen Fu, Jie Wen *, Zhi Tao, Guoqiang Xu, Haoran Huang

National Key Laboratory of Science and Technology on Aero-Engine Aero-thermodynamics, Collaborative Innovation Center of Advanced Aero-Engine, School of Energy and Power Engineering, Beihang University, Beijing 100191, China

HIGHLIGHTS

- U-turn tube bending section has 40% ~ 2 times HTC larger than that in the straight tube section.
- "Sine curve" wall temperature distribution appears due to the coupling effect between centrifugal force and buoyancy.
- Heat transfer enhancement increases with the decrease of bending diameter.
- $Gr_q/Gr_{th} > 2$ could be one criterion to evaluate buoyancy effect for supercritical hydrocarbon fuel flowing in U-turn tubes.

ARTICLE INFO

Article history:
Received 16 November 2016
Revised 3 January 2017
Accepted 15 January 2017
Available online 18 January 2017

Keywords:
Supercritical
Convective heat transfer
U-turn tubes
Centrifugal force
Buoyancy

ABSTRACT

Convective heat transfer characteristics of hydrocarbon fuel RP-3 flowing through U-turn tubes at supercritical pressures were experimentally investigated. The inner diameter of U-turn tubes is 1.82 mm and bending diameters are 20 mm, 30 mm and 40 mm. Inner wall temperature and HTC variations were analyzed under different physical factors including heat flux, system pressure, bending diameter and flow direction. Test results indicate that centrifugal force strengthens the flow mixing at the bending section and HTC is averagely enhanced by 40% to twice compared with straight tube. In addition, HTC values increase with decrease of bend diameter and variation curves of all U-turn tubes are displayed as "Inverted U" type. Finally, $Gr_q/Gr_{th} > 2$ is concluded as one criterion evaluating buoyancy effect for supercritical hydrocarbon fuel flowing in U-turn tubes.

1. Introduction

From the perspective of engineering thermodynamics, two main ways are considered to improve the aircraft engine performance: increasing the engine turbine inlet temperature and compressor pressure ratio. However, the improvement of technical parameters would face severe challenges of high temperature heat load from outlet air temperature. According to the heat load and cooling problem in aircraft engine, academic circles put forward the CCA (Cooled Cooling Air) technology [1] which is suitable for high performance aero-engine turbine components. CCA technology refers to the heat exchanger installation on the aircraft engine, with the aircraft's own hydrocarbon fuel as cold source in advance. The hot side will be turbine cooling air of high temperature components and the heat exchange equipment would improve the cooling quality of the cooling air. As the fuel feed system varies from 3.45 to 6.89 MPa in typical aero engine [2], hydrocarbon fuel would be heated and compressed in the supercritical status. Hence, flow and heat transfer characteristics should be clearly obtained for aero-engine application.

Previous researches of supercritical fluid heat transfer mainly focus on pure liquids such as water, carbon dioxide and some refrigerating fluids. These investigations are based on the application of supercritical boiler generator [3,4], membrane contactors [5,6] and nuclear reactor technology [7,8]. Jackson and Hall [9] analyzed the mechanism of heat transfer enhancement and deterioration for supercritical fluid flowing in different directions. The wall temperature is higher than fluid bulk temperature at heating conditions and temperature gradient in the radial direction could occur buoyancy due to the thermal properties variations. Also, the turbulence energy is the main factor to trigger the heat transfer enhancement or deterioration. A dimensionless criterion Bo^* defined as $Bo^* = Gr^*/(Re^{3.425}Pr^{0.8})$ was proposed to predict the buoyancy influences on heat transfer and enhancement happens in the downward flow conditions. In the following research work

* Corresponding author.
E-mail address: wenjie@buaa.edu.cn (J. Wen).

http://dx.doi.org/10.1016/j.applthermaleng.2017.01.058
1359-4311/

Nomenclature

A	surface area (m^2)
Bo^*	buoyancy factor
C_p	isobaric specific heat capacity (kJ/(kg K))
d	diameter (m)
G	mass flow rate (kg/(m^2 s))
Gr	Grashof number
H	enthalpy (kJ/kg)
h	heat transfer coefficient (W/(m^2 K))
I	electrical current (A)
L	length (m)
m	mass flux (g/s)
Nu	Nusselt number
P	pressure (MPa)
Pr	Prandtl number
Q	heat (W)
q	heat flux (kW/m^2)
Re	Reynolds number
$R(T)$	electronic resistivity (Ω m)
r	radius (m)
T	temperature (K)
U	voltage (V)

Greek

Φ	heat power (W)
ρ	density (kg/m^3)
μ	dynamic viscosity (Pa s)
ν	kinetic viscosity (m^2/s)
λ	thermal conductivity (W/(m K))
β	thermal diffusivity (m^2/s)

Subscripts

b	bulk
i	inner
o	outer
pc	pseudo-critical
q	heat flux
th	thermal
w	wall
x	local position

about supercritical fluid heat transfer in vertical circular tube, similar results were observed. Petukhov [10] and Majid Bazargan [11] both investigated supercritical water heat transfer characteristics flowing in horizontal tubes. The criterion of $Gr_q < Gr_{th}$ could judge the buoyancy influence level in horizontal flow. Besides the buoyancy effect, the thermal acceleration could also induce the heat transfer deterioration in different mechanism compared with buoyancy [12,13]. Shiralkar and Griffith [14,15] experimentally studied convective heat transfer of supercritical CO_2 flowing in a 2 mm circular tube and the results demonstrate that there exist wall temperature peaks in both upward and downward flow. McEligot [16] and Jackson [17] analyzed that the bulk fluid density decreased to make the turbulent flow relaminarization and then deteriorated the heat transfer. Moreover, Liao [18,19] and Jiang [20–22] systematically studied the supercritical CO_2 heat transfer flowing in micro-tubes with various diameters. The results show that the heat transfer deterioration occurs in the section of pseudo-critical point when the Reynolds number is higher than 10^5. Tube diameter could significantly affect heat transfer characteristics on the basis of various wall temperature distributions along the tube.

Compared with pure liquid, heat transfer for hydrocarbon fuel is more complicated due to the mixture of hydrocarbons and chemical reactions. John Holland Kriegert [23] used SF6 to replace aviation kerosene to study heat transfer coefficient variation at different factors. The results illustrate that system pressure and flow direction have little influence on heat transfer when the Reynolds number is lower than 10,000. However, system pressure could change the heat transfer coefficient variation at high Reynolds number conditions. Linne [24,25] experimentally investigated thermal stability and heat transfer characteristics of supercritical JP-7 in a 2.42 mm circular tube. In all experimental tubes of different materials, thermal instability likes nucleate boiling and heat transfer enhancement happened with the increase of heat flux. It is also noted that the increasing inlet temperature could reduce the thermal instability and there exists strong buoyancy effects in all experiments. Hitch and his team [26,27] studied flow and heat transfer of supercritical JP-7 and MCH flowing in vertical tubes. The experimental phenomena indicate that buoyancy force could lead to the mixed convection at the pseudo-critical section when the pressure is twice larger than critical pressure.

For researches about flow and heat transfer of supercritical fluid, most of them were experimented and simulated in straight circular tubes. Some typical reviews about supercritical fluid heat transfer have been published by Pioro [28,29], Duffey [30], and Yoo [31] several years ago. However, researches about Chinese typical aviation kerosene RP-3 are being carried out more and more, such as thermal property measurements [32–35], convective heat transfer [36–39], and flow resistance characteristics [40]. Furthermore, much more researches [41–44] focus on the thermal oxidation and cracking influences on flow and heat transfer of aviation kerosene RP-3. To consider the real application for air-fuel heat exchanger in aero engines, heat transfer mechanism of supercritical hydrocarbon fuel flowing through curved tubes is vitally important. Thus, convective heat transfer of aviation kerosene RP-3 flowing in U-turn tubes at supercritical pressures is chosen to study and some meaningful results are conducted in this paper.

2. Experimental

2.1. Test facility

Fig. 1 shows the schematic of supercritical fluid flow and heat transfer system in Beihang University. The whole system consists of three main sub-systems: preparative system, measured system and reclaim system. In preparative system, the fuel in the tank is pumped up to fixed system pressure by a metering pump (SP6015, 15 MPa; 0.01-600 ml/min). The fuel from the pump is divided into a major path fuel and a bypass fuel. The bypass fuel was collected to reuse and one valve was set to control the system pressure. Then the fuel mass flow rate was measured using a Coriolis-force flow meter (Model: DMF-1-1, 0.15%, Sincerity) and its value was also adjusted by the metering pump. In order to achieve the required inlet temperature of the test section, two pre-heaters were connected after the flow meter which were independently controlled by DC power supplies with 20 kW capacity.

The system static pressure was measured by a pressure gage transducer (Model 3051CA4, Rosemount) at the inlet of test section. Two K-type sheathed thermocouples were inserted through joints to measure the inlet and outlet fuel temperatures. After

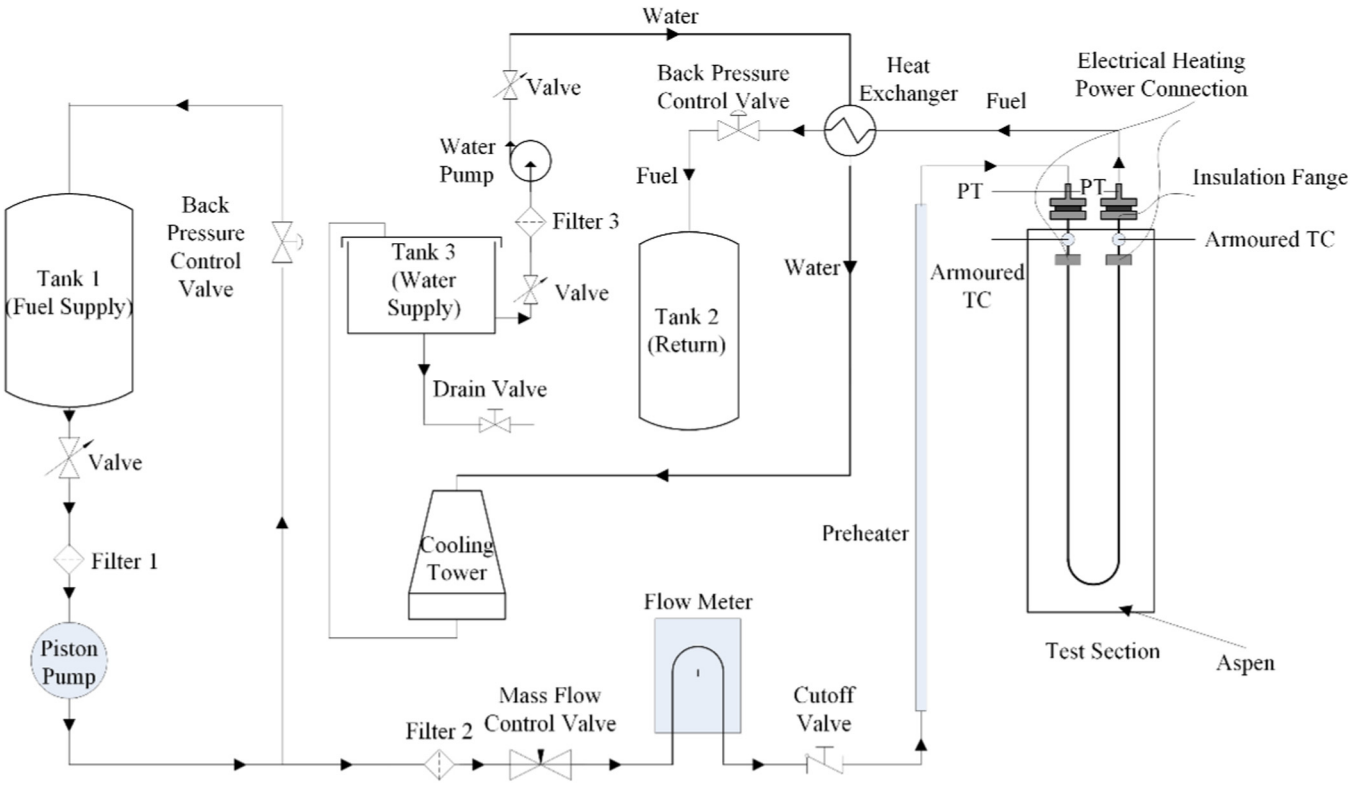

Fig. 1. Schematic of experimental system.

the measured system, the hot fuel was cooled down to room temperature by fuel-water cooler and then collected to the waste fuel barrels. All the measured experimental data were output in the form of electrical signals, including absolute pressure, temperature, mass flow rate, heating voltage and current. The signal was gathered by ADAM-4018 data acquisition, transformed by ADAM-4520 to several documents and stored in the computer.

2.2. Test section

The experimental test section is stainless steel (1Cr18Ni9Ti) tube with 1.82 mm inner diameter and 0.19 mm wall thickness. All U-turn tubes are silver welded with stainless steel joint to reduce the local pressure drop. The experimental tube has the length of 800 mm with 500 mm heating section. In order to guarantee flow full development in the experimental section, 150 mm (L/d = 82.4) adiabatic sections are set aside both in the inlet and outlet zones. Three different types of U-turn tubes with bend diameters of 20 mm, 30 mm and 40 mm were fabricated in the identical full length.

There are 25 K type thermocouples non-uniformly welded onto the outer wall of the experimental tube to test the wall temperatures. Fig. 2 shows the thermocouple distributions along the U-turn tube and four thermocouples are distributed uniformly on the cross section of bending center. The whole test section is covered by insulating material called Aspen. All the wide range of experimental parameters are displayed in Table 1.

2.3. Data reduction

The local heat transfer coefficient (HTC) h_x is calculated by the following equation.

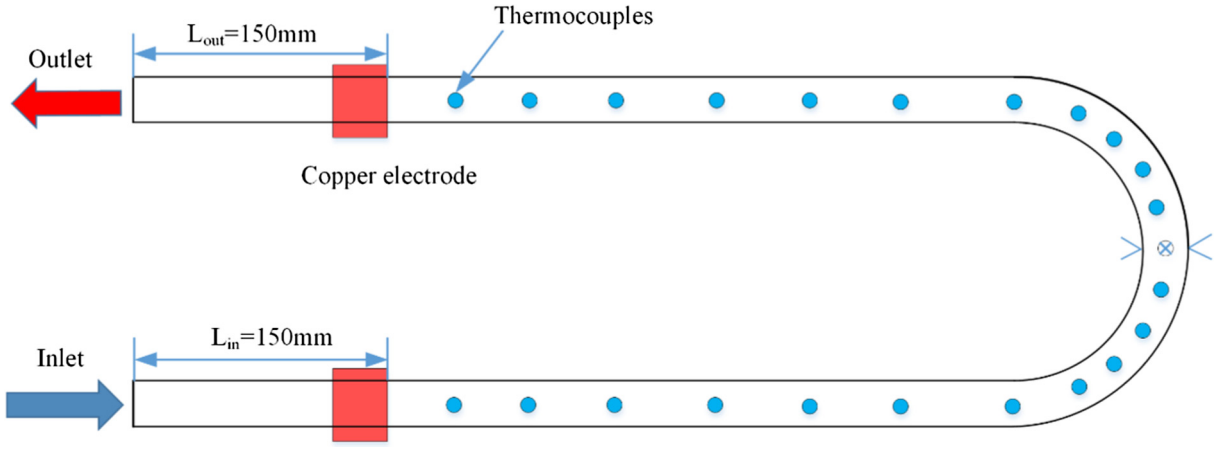

Fig. 2. Thermocouples distribution of test U-turn tube.

Table 1
U-turn tubes parameters and experimental conditions.

U-turn tube parameters		Experimental	Range
Inner diameter (mm)	1.82	System pressure (MPa)	3, 4, 5
Heated length (mm)	500	Mass flux (kg/m^2 s)	589–1375
Bending diameter (mm)	20	Heat flux (kW/m^2)	50–700
	30	Inlet temperature (K)	373–633
	40	Flow directions	Horizontal, up-down, down-up

Table 2
Measured Instruments and precisions.

Measured parameters	Instruments	Precisions
Inner diameter	Scanning Electron Microscope	±0.0005 mm
Mass flux	Coriolis force mass flow-meter	±0.15%
Fuel temperature	K type armored thermocouple	±0.5 K
Outer wall temperature	K type thermocouple	±0.5 K
Current	Ampere meter with output	±0.2%
Voltage	Voltmeter with output	±0.2%

$$h_x = \frac{q_x}{T_{wx,in} - T_{bx}} \tag{1}$$

where q_x is effective heat flux onto the outer wall and it could be defined by

$$q_x = \frac{I^2 R(T)/[\pi(d_{out}^2 - d_{in}^2)/4]}{\pi d} - q_{loss,x} \tag{2}$$

$R(T)$ is electrical resistivity of the stainless steel tube. $q_{loss,x}$ is heat losses and the calibration should be done for each U-turn tube.

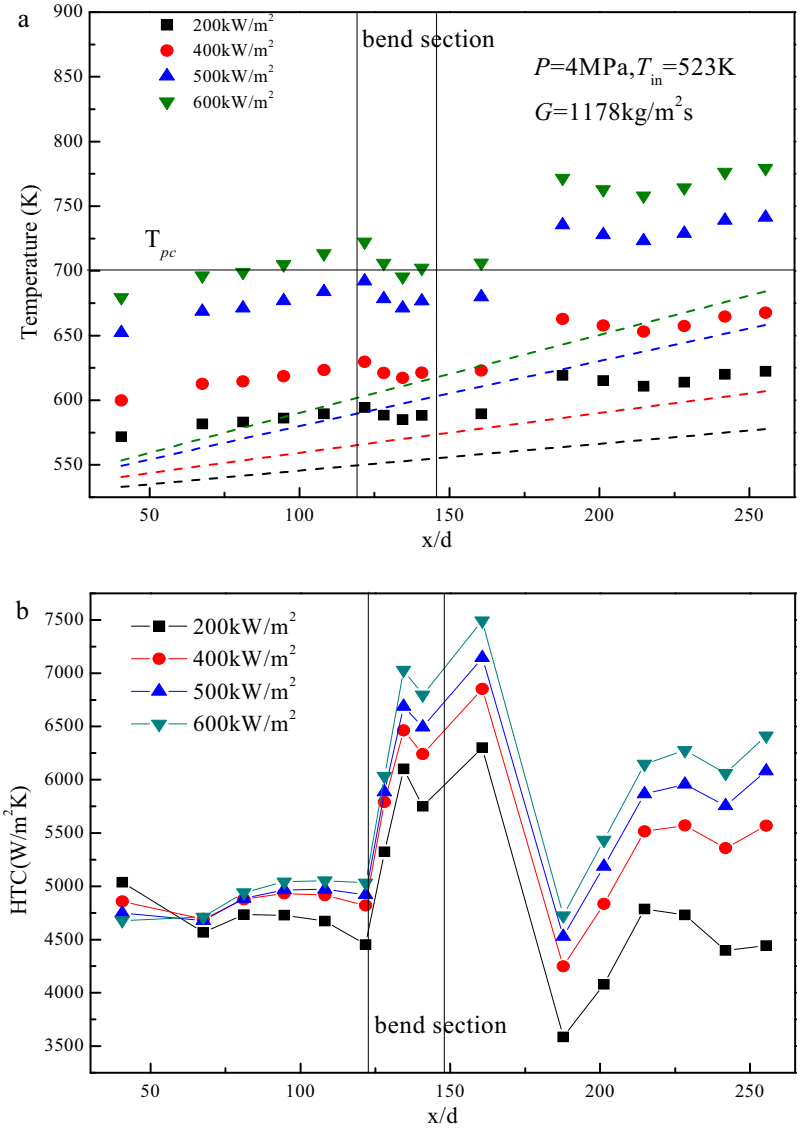

Fig. 3. Temperature and HTC distributions under various heat fluxes.

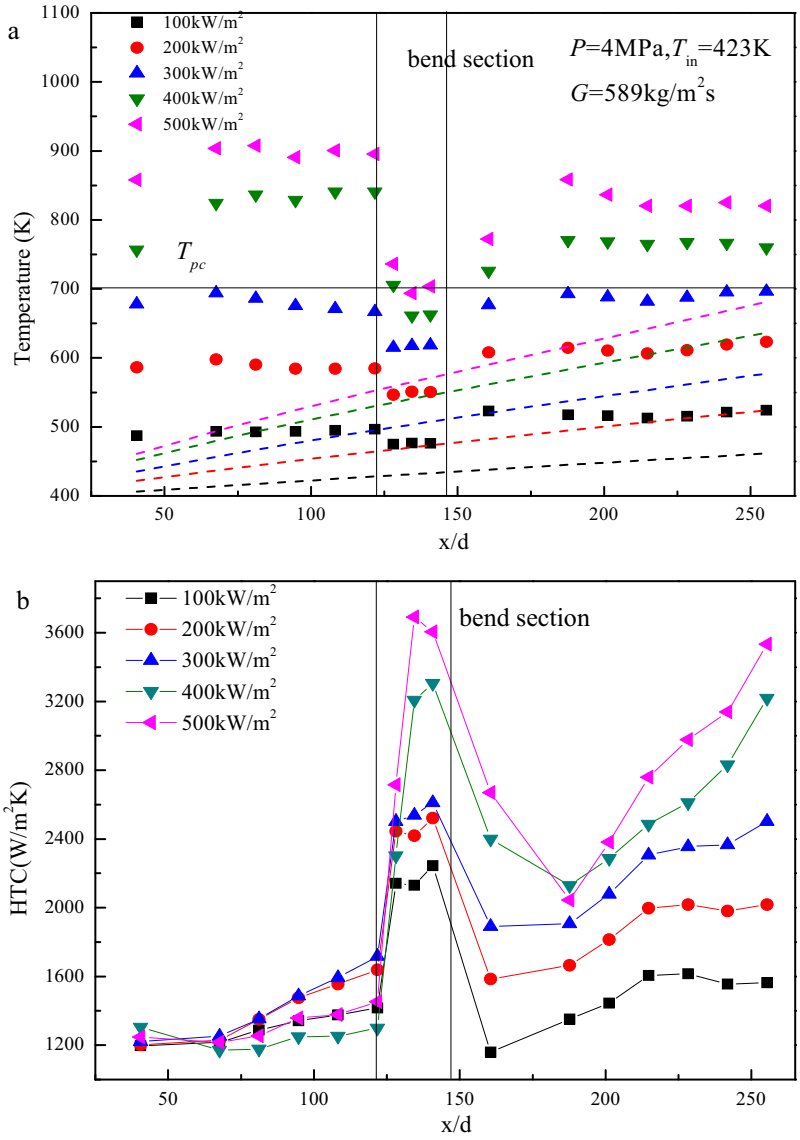

Fig. 4. Temperature and HTC distributions at low inlet Reynolds numbers.

The local fuel temperature $T_{b,x}$ is determined by the relationships among the local heat flux, the inlet and outlet fuel enthalpy, which have been measured in previous research [45]. The inner wall temperature is calculated by solving the 1-D thermal conductivity equation at the cylindrical coordinate system as follows

$$\frac{\lambda}{r}\frac{\partial}{\partial r}\left(r\frac{\partial T}{\partial r}\right)+\dot{\Phi}=0 \tag{3}$$

The boundary conditions are

$$r=r_o,\quad \lambda\frac{\partial T}{\partial r}=q_{loss}(r) \tag{4}$$

Then $T_{wx,i}$ could be obtained by

$$T_{wx,i}=T_{wx,o}-\left[\left(\dot{\Phi}\frac{r_o^2}{2}-q_{x,loss}r_o\right)\ln\frac{r_o}{r_i}-\frac{\dot{\Phi}}{4}(r_o^2-r_i^2)\right]\Big/k_x \tag{5}$$

where $T_{wx,i}$ and $T_{wx,o}$ represent inner and outer wall temperatures of the experimental tube. $\dot{\Phi}$ is power produced by per unit volume of tube resistance and k_x is local thermal conductivity of the U-turn tube.

Table 2 shows the measured parameters and instruments precisions. As the minimum temperature difference between the inside wall and the bulk fuel is 30 K, the uncertainties of local wall temperature and fuel temperature are ±1.05 K and ±0.85 K. Also, the uncertainty of the effective heat flux is 2.7% due to the heat loss calibration. According to the error transfer formula, the maximum uncertainties of HTC is defined as ±5.2%.

3. Results and discussion

3.1. Effect of heat flux

Fig. 3 shows the inner wall temperature, fuel bulk temperature and HTC distributions for horizontal U-turn tubes. The experimental condition is 4 MPa system pressure, 523 K inlet temperature and 1178 kg/m² s mass flux. The straight horizontal line in the graph represents the pseudo-critical temperature. To evaluate the equivalent heat transfer variation, the temperature measuring points were set in the same plane of U-turn tube parallel to the ground. The results show that the temperature gradient between the fluid and the wall is large in the entrance area of the

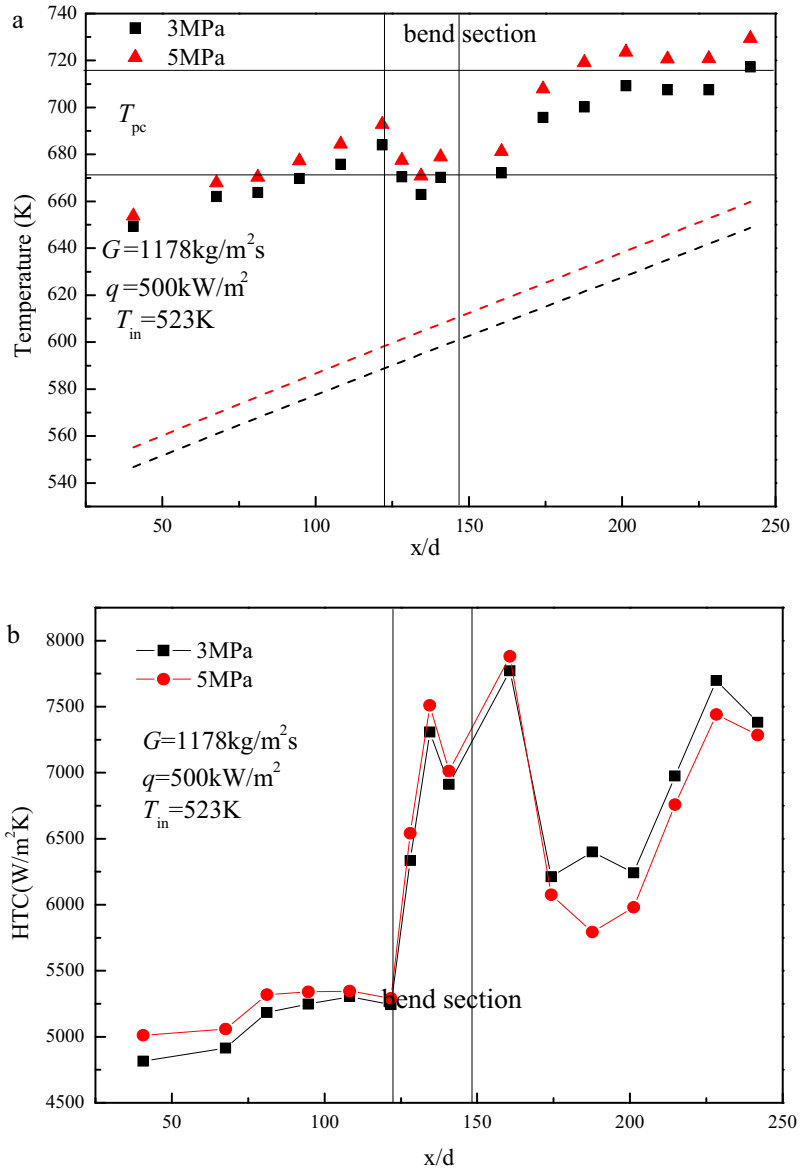

Fig. 5. Temperature and HTC distributions at various system pressures.

experimental section. Buoyancy force weakens the wall shear stress and then causes flow "relaminarization" near the wall. Thus, heat transfer deterioration phenomena occur and the extent gets stronger with the increase of heat flux. The average wall and fuel bulk temperatures are increasing as the fuel flows through the tube. Also, isobaric heat capacity increase and viscosity decline would lead the heat transfer to recover to the normal level.

After entering 180° bend area, the fuel flow is motivated by centrifugal force and makes flow disturbance more disorder. Then turbulence intensity is strengthened to trigger wall temperature drop in this area, and convective HTC increases by about 40% compared with straight area. As fuel flow has been changed to the opposite direction, the fluid boundary layer develops again and the second "entrance effect" occurs. HTC at the dimensionless location from x/d = 160 to 210 are in the range from deterioration to recovery and HTC values remains stable along the tube at the same heat flux. The increase level of wall temperature starts to slow down with the increase of heat flux at the outlet section and HTC slowly increases along the tube.

Heat transfer characteristics are shown in Fig. 4 as experimental inlet Reynolds number was set in the lower level. The results indicate that heat transfer significantly deteriorates at heat flux conditions of 400 and 500 kW/m^2 before the bending section due to the lower turbulence kinetic energy. At the dimensionless position x/d from 0 to 120, the HTC values are in the range between 1200 kW/m^2 K and 1700 kW/m^2 K. The near wall temperature is higher than pseudo-critical temperature and temperature difference could lead strong buoyancy influences, and then heat transfer deterioration occurs. At the bending section, centrifugal force influence is much stronger than buoyancy effect and wall temperature "trough value" appears in the center of the bend. Moreover, HTC increases twice larger than that in the straight tube section at the heat flux condition of 500 kW/m^2.

3.2. Effect of system pressure

Fig. 5 displays inner wall temperature, fluid bulk temperature and local HTC variations to compare system pressure effect between 3 MPa and 5 MPa. At the inlet straight tube section, most of inner wall temperatures are between pseudo critical temperatures 669.8 K and 716.3 K. Thus, no obvious difference of HTC variation could be obtained for two pressures. With the increase

of fluid bulk temperature, the variation of thermal properties near to the critical temperature is more severe and isobaric specific heat capacity peak value of 3 MPa is much higher than 5 MPa as shown in Fig. 6. It is shown in Fig. 5b that HTC value in 3 MPa is mostly larger than that in 5 MPa when the dimensionless temperature T_b/T_{pc} is higher than 0.95. Significant variation of thermal properties plays the key factor to influence heat transfer distribution under different system pressures. Isobaric specific heat capacity value of 5 MPa is higher than 3 MPa by about 40%, thermal conductivity is less than 10%, and basically density value remains the same. The thermal diffusivity $\frac{\lambda}{\rho C_p}$ at 3 MPa leads to enhancements of fluid momentum and thermal diffusion ability. Hence, the outlet straight tube section has smaller temperature difference between bulk fluid and wall, and then the heat transfer is enhanced.

3.3. Effect of inlet Reynolds number

Mass flux variation could induce the variation of buoyancy in the straight tube section and also affect heat transfer leading by centrifugal force in the bending section. Inner wall temperature and HTC variations of different mass fluxes at 4 MPa conditions are shown in Fig. 7. The results demonstrate that inner wall temperatures at lower inlet Reynolds numbers conditions are nearly 200 K larger than the pseudo-critical temperature (701.2 K) and fluid bulk temperature. The inlet effect could restrain the HTC increase and leads to the increase of wall temperature. With the increase of main flow temperature, the turbulent kinetic energy could wear off the influence of buoyancy and recover the heat exchange ability. The increase of inlet Reynolds number makes an overall increase of turbulent kinetic energy and there appears no obvious heat transfer deterioration at the inlet straight tube section.

However, heat transfer enhancement is significantly observed for all working conditions in the bending section. Centrifugal force induced by bending could lead to stronger mixing between flow boundaries and then strengthen convective heat transfer. At the central area of bending section, HTC for low Reynolds number condition is basically consistent. With the increase of bending section Reynolds number, the ability of inner wall decline tends to level off and heat transfer enhancement returns to the normal level.

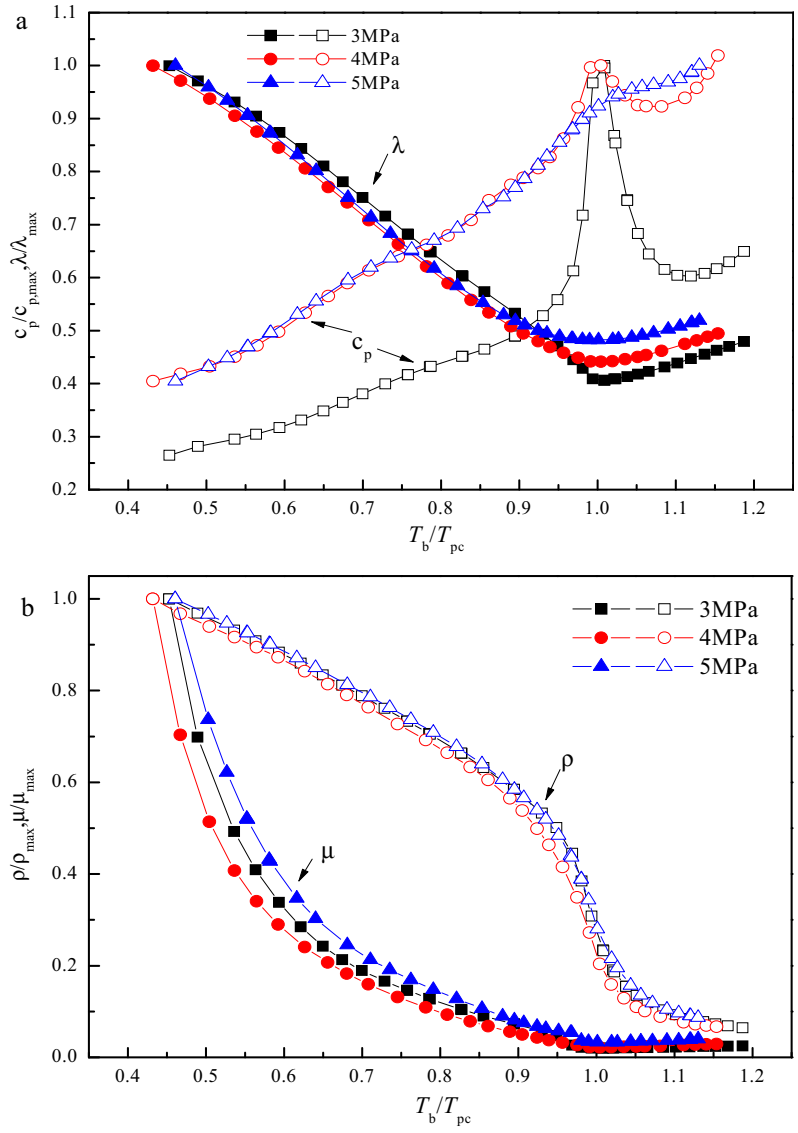

Fig. 6. Hydrocarbon fuel thermal properties variation at different pressures.

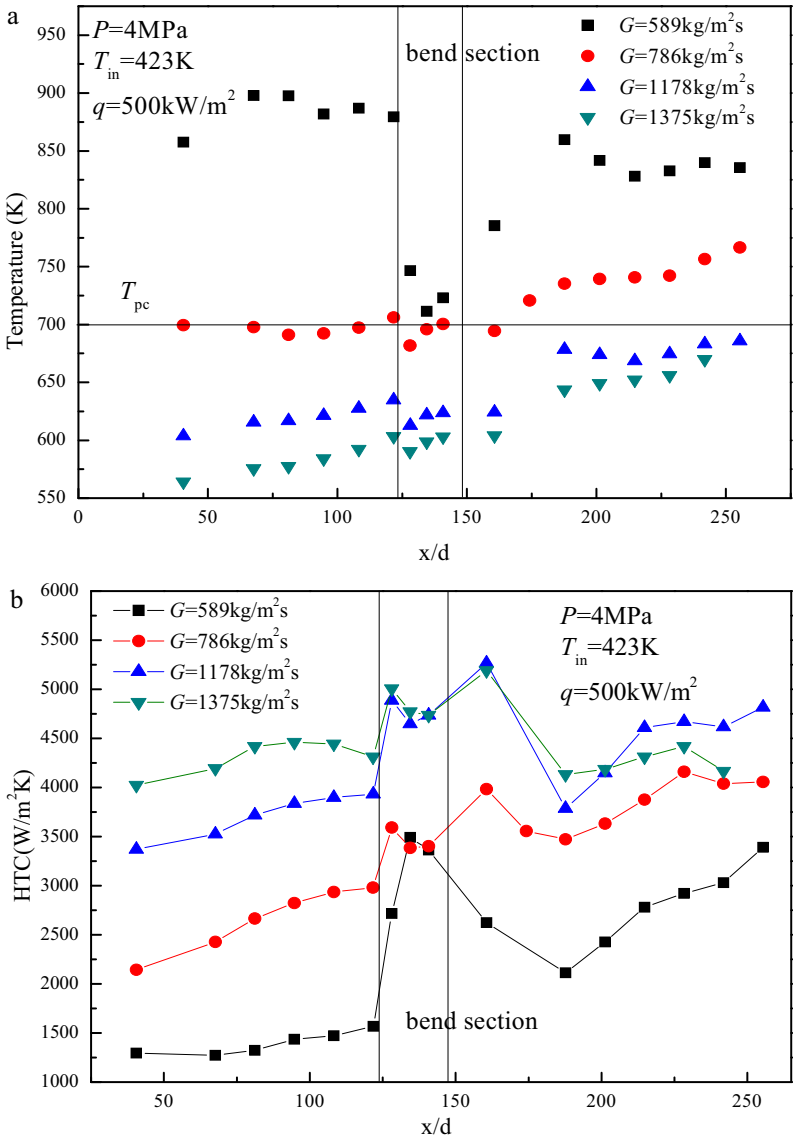

Fig. 7. Temperature and HTC distributions at various mass fluxes.

3.4. Effect of bend diameter

As bend diameters of U-turn tubes are different, centrifugal forces induced are various to distinguish heat transfer characteristics. Fig. 8 shows inner wall temperature, fuel bulk temperatures and local HTC variations for different U-turn tubes. It is noted that the bending diameter could influence the whole main flow pattern and leads to the inner wall temperatures different distributions. Obvious entrance effects are observed for three kinds of U-tubes due to the boundary layer development and increasing thickness. Density difference between the mainstream and the near wall layer increases. And then the gravitational buoyancy lift has affected the wall shear stress distribution to deteriorate the heat transfer. Under the same entrance condition, centrifugal force plays a leading role in the bending section. Heat transfer enhancement is observed compared with straight tube section. It is explained that the secondary flow induced by centrifugal force moves outside and strengthen the turbulent mixing. The unit fuel is motivated by the centrifugal force u^2/r and the smaller bending radius could make larger perturbation kinetic energy. Thus, 20 mm U-turn tube has the lowest wall temperature and highest HTC variations as shown in Fig. 8.

Fig. 8b shows that bending section temperature distribution could influence the HTC at the straight tube section. For U-turn tube with 40 mm bending diameter, maximum HTC at the bending section is about 3 times larger than that at the straight tube section. However, these value are only 1.75 and 1.67 times for 30 mm and 20 mm U-turn tubes. It could be explained that larger bending diameter influence the fluid bulk temperature in the wide range and inner wall temperature difference is declined between the bending and straight sections. Centrifugal force increase the density gradient near the wall and decrease the boundary layer adhesion. Thus, heat transfer obviously enhances and HTC for all bending diameters shows “Inverted U” type distributions.

3.5. Effect of flow direction

In order to evaluate flow direction effects on heat transfer, U- turn tubes were set in two different vertical ways: up-down and down-up. Fig. 9a shows inner wall temperature variations for different flow directions that buoyancy slightly influence heat transfer to make inner wall temperatures in the same level. As compressed fuel flows into the circular tube with the developing boundary layer, the entrance effect leads to the temperature peak

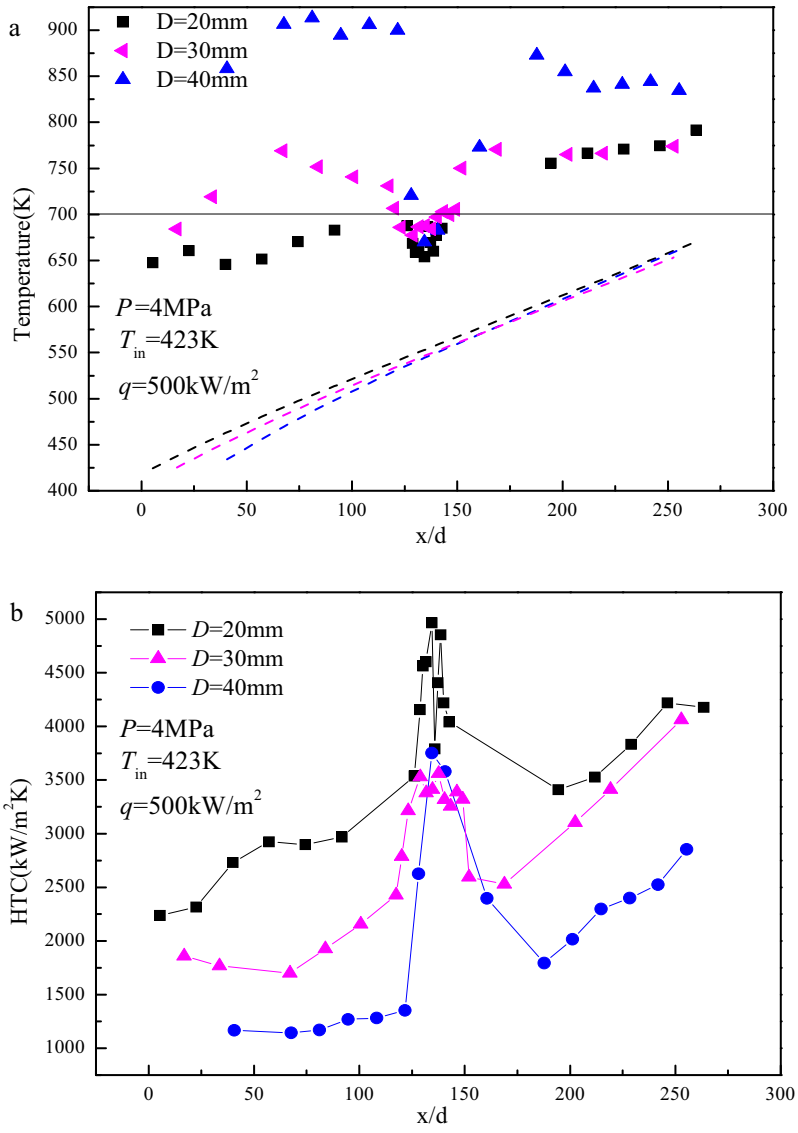

Fig. 8. Temperature and HTC distributions at various bending diameters.

of upward flow to deteriorate the heat transfer. For 400 kW/m^2 and 500 kW/m^2 heat flux conditions, isobaric specific heat capacity peak enhance the heat transfer in the region of pseudo critical temperature under the condition of downward flow. Moreover, heat transfer difference of different flow directions are mainly due to the directions of flow and buoyancy. Density and viscosity variations affect the velocity type of supercritical fuel, and in turn to affect the thermal boundary layer development to induce inner wall temperatures variations because of comprehensive buoyancy lift. However, flow direction could not significantly deteriorate heat transfer as centrifugal force plays the key point in the bending section.

HTC variations for horizontal and vertical flows are displayed in Fig. 9b. It is seen from the figure that HTC maximum value appears at the bending center point for vertical flows. The reason is that gravitational and centrifugal buoyancy couples at the same level and heat exchange capacity strengthens near the center. For horizontal flow, gravitational buoyancy is perpendicular to the centrifugal force and the maximum coupling effect turns to the downstream of the fuel flow direction. In addition, the second entrance effect on the outlet straight tube section could be inhibited due to the mixing by gravity and centrifugal force for the vertical flow. As significant entrance effect is observed for the horizontal flow, HTC decreases to the minimum value and then slowly recovers to the regular heat transfer.

3.6. Combined effect of centrifugal and buoyancy forces

As centrifugal force and buoyancy effect exist during the supercritical flow of hydrocarbon fuel in horizontal U-turn tubes, distribution inhomogeneity of circumferential wall temperature is significantly observed. To evaluate the above phenomena, 4 groups of NiCr-NiSi thermocouples are uniformly welded on the dimensionless position of x/d = 134.4, corresponding to the bending section center. Fig. 10 shows the thermocouple positions including bottom(0°/360°), inside(90°), top(180°) and outside(270°). The working heat flux varies from 100 kW/m^2 to 500 kW/m^2 and circumferential inner wall temperature distributions for different mass flux are shown in Fig. 11. The results demonstrate that circumferential wall temperature distribution presents as 'Standard Sine' curve. Inside wall temperature is the highest, outside value is the lowest, and the top and the bottom wall temperatures are at the basic level. It is explained that the centrifugal force mainly leads to the temperature difference between inside and outside.

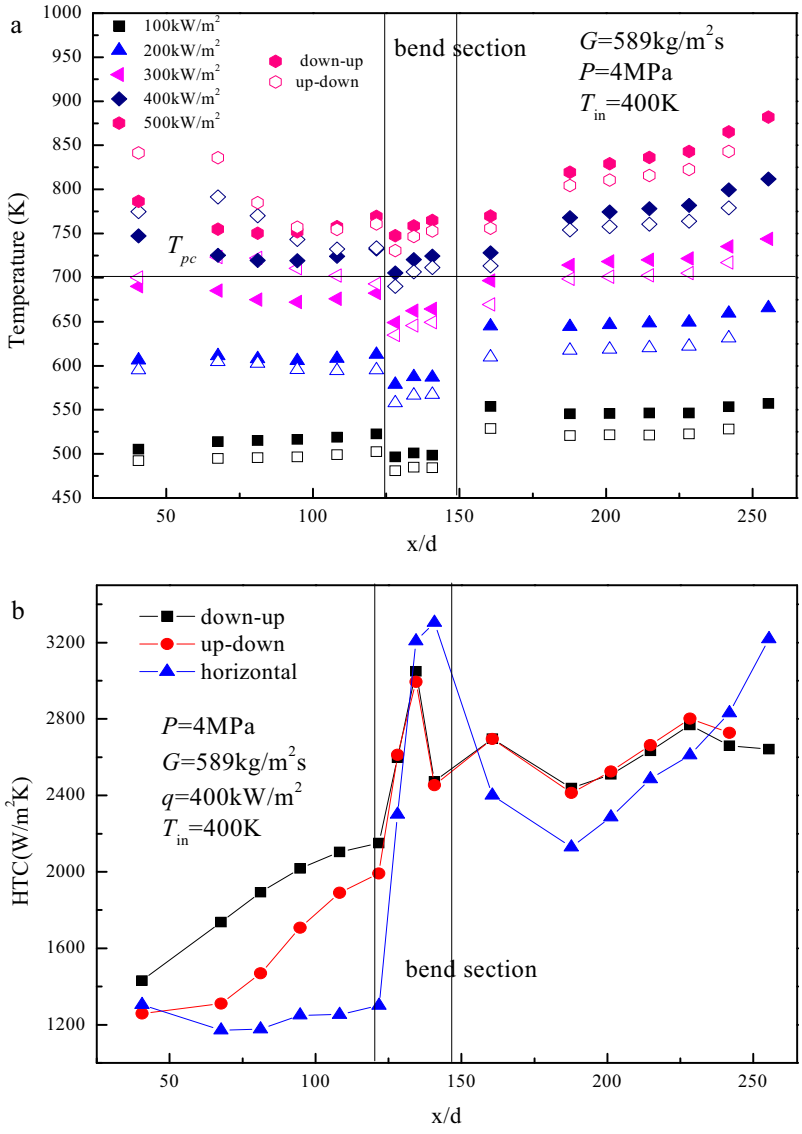

Fig. 9. Temperature and HTC distributions at various flowing directions.

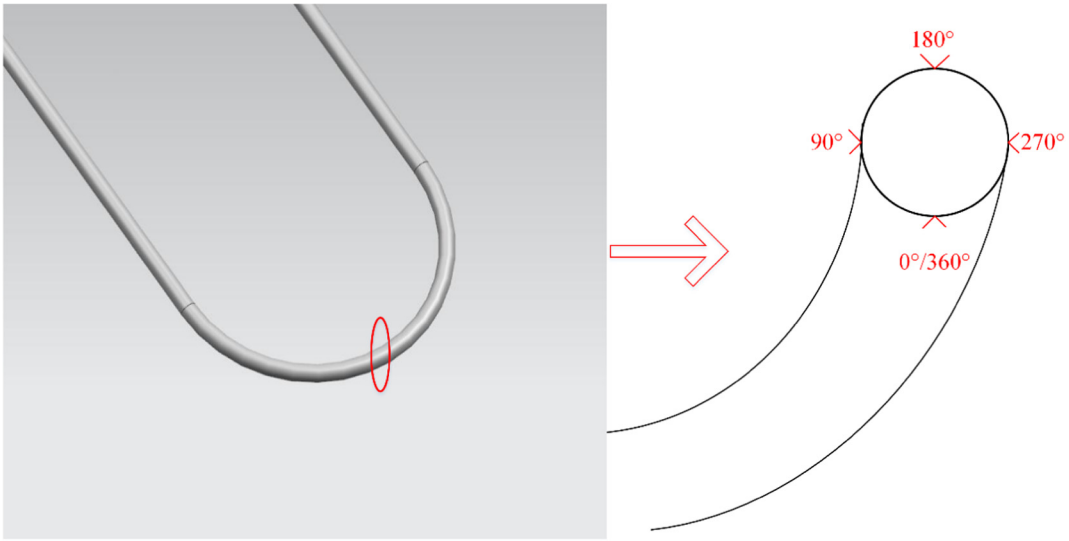

Fig. 10. Thermocouples distributions at the bending center.

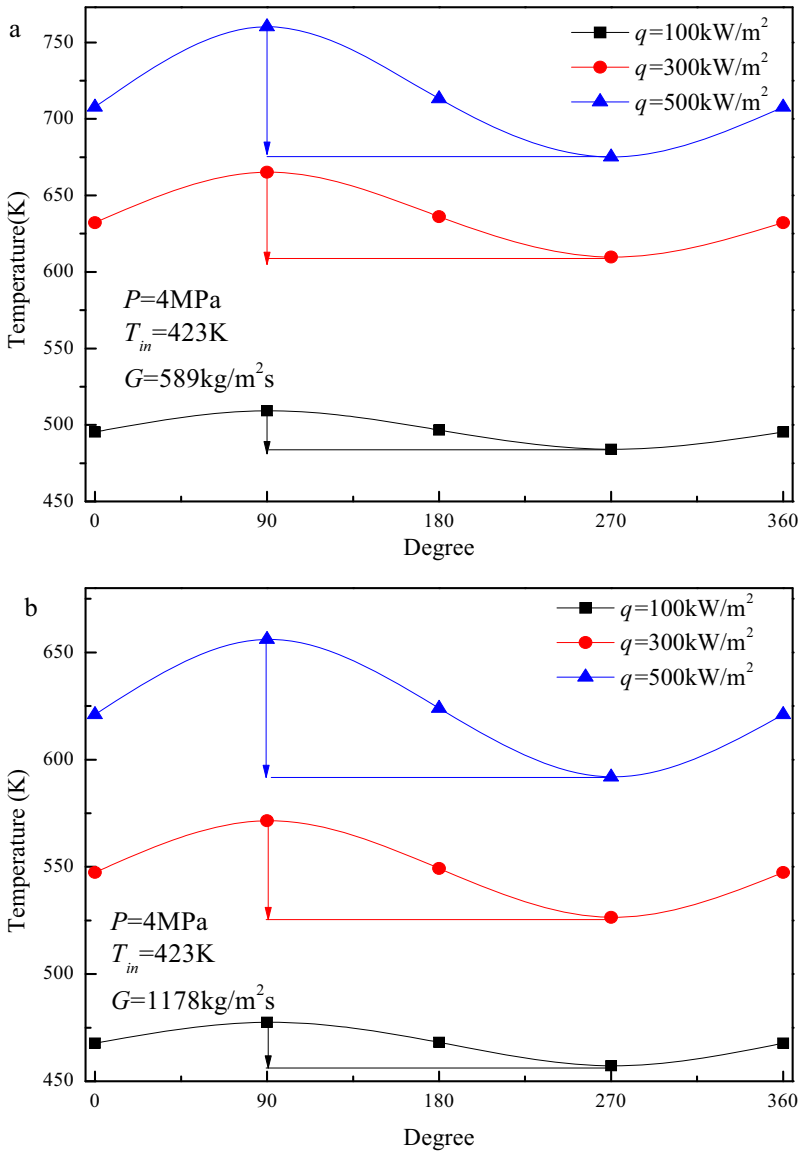

Fig. 11. Inner wall temperature variations at the same cross section.

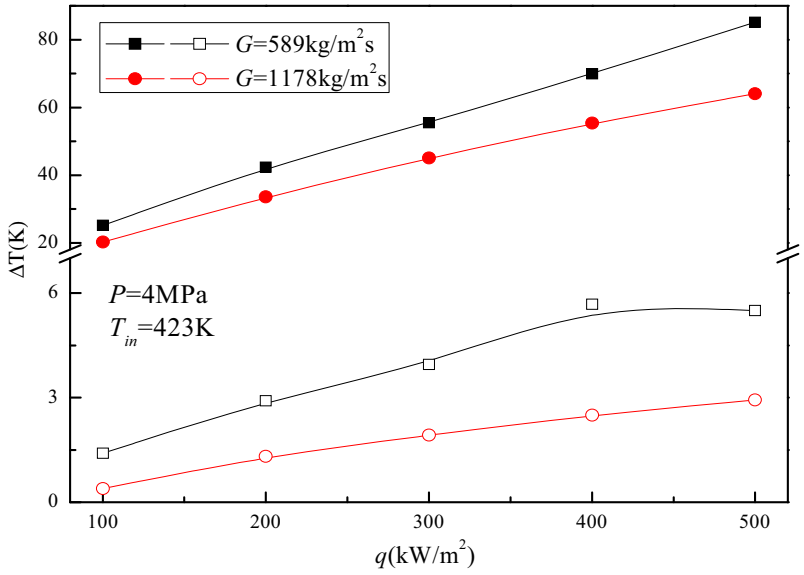

Fig. 12. Two temperature difference distributions along with heat flux.

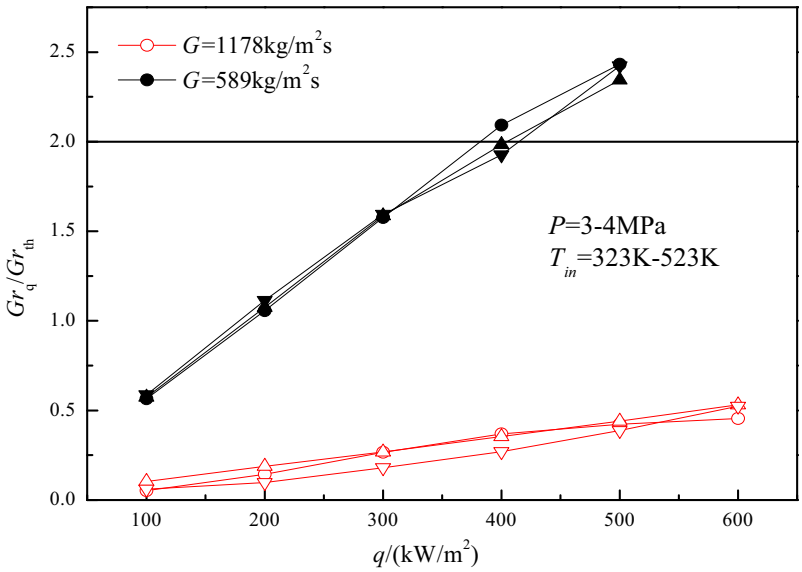

Fig. 13. Buoyancy criterion distributions along with heat flux.

Furthermore, Fig. 12 shows temperature differences between the inside and outside (solid point line), and between the top and bottom (hollow point line) variations along with heat flux. It is displayed in the figure that two kinds of wall temperature differences gradually change with the tendency of linear growth.

As mainstream flow heat flux increases, fuel density and viscosity decrease with the increase of fuel temperature. The main flow velocity sharply increases when the mass flux is kept as constant. Then the centrifugal acceleration starting to change the wall temperature distribution. The figure shows that the inside wall temperature is always larger than the outside and temperature difference increases from 20 K to 80 K, which is significant for circular tube with 1.82 mm inner diameter. Nevertheless, the temperature difference between top and bottom is within 6 K and buoyancy effect could be ignored under these two working conditions. Petukhov [10] proposed dimensionless number Gr_q/Gr_{th} to judge the buoyancy influence in the horizontal circular tube flow as follows:

$$Gr_q = \frac{g\bar{\beta}q''d^4}{v_b^2\lambda_b} \tag{6}$$

$$Gr_{th} = 3\times10^{-5}Re_b^{2.75}\overline{Pr}^{0.5}[1+2.4Re_b^{-1/8}(\overline{Pr}^{2/3}-1)] \tag{7}$$

$$\overline{Pr} = \frac{i_w - i_b}{T_w - T_b}\frac{\mu_b}{\lambda_b} \tag{8}$$

$$\overline{\beta} = \frac{1}{\rho_{film}}\frac{\rho_b - \rho_w}{T_w - T_b} \tag{9}$$

Fig. 13 shows the correlation value variation along with heat flux at the dimension-less position x/d = 134.4 for all experimental conditions. The results conclude that the values of Gr_q/Gr_{th} are all less than one for high mass flux conditions and buoyancy effect could not be considered. When the mass flux is 589 kg/m^2 s, increasing tendency of temperature difference between top and bottom begins to appear gently. The starting point corresponding to the value of Gr_q/Gr_{th} is about 2 and secondary flow induced by buoyancy is starting to influence wall temperature distribution. According to RC. Xin [46] research, the coupling effect between centrifugal force and buoyancy could let the highest wall temperature shift to the section of 90–180° at the same transverse plane. In a word, $Gr_q/Gr_{th} > 2$ could be used to judge the buoyancy effect on the bending section of supercritical hydrocarbon fuel heat transfer in U-turn tubes.

4. Conclusion

Convective heat transfer characteristics of supercritical hydrocarbon fuel RP-3 flowing through U-turn tubes were experimentally investigated. Heat flux, system pressure, bending diameter and flow directions effects on heat transfer were analyzed. Also, buoyancy combined with centrifugal force influences on convective heat transfer were considered and the following conclusions were obtained.

(1) Centrifugal force could strengthen the flow mixing at the bending section and this enhances the HTC by 40% to 2 compared with straight tube. The highest HTC value appears at the bottom center of the bending section.
(2) Second “entrance effect” happens at the outlet straight tube section for horizontal flow and the heat transfer ability starts to recover to the normal level.
(3) With the decrease of bending diameter, flow centrifugal force increases and heat transfer enhances. All U-turn tubes HTC variation curves are displayed as “Inverted U” curves.
(4) Coupling effect between centrifugal force and buoyancy influences the wall temperature distribution. $Gr_q/Gr_{th} > 2$ is summarized as one criterion to evaluate buoyancy effect for supercritical hydrocarbon fuel in U-turn tubes.

Acknowledgement

The authors would like to acknowledge the financial support provided by the China National Natural Science Foundation (Grant NO. 51606179).

References

[1] G. Bruening, W. Chang, Cooled Cooling Air Systems for Turbine Thermal Management, ASME Paper, (99-GT), 1999, p. 14.
[2] H. Huang, L.J. Spadaccini, D.R. Sobel, Fuel-cooled thermal management for advanced aeroengines, J. Eng. Gas Turb. Power 126 (2) (2004) 284.

[3] S. Zheng, Z. Luo, H. Zhou, Distributed parameter modeling and thermal analysis of a spiral water wall in a supercritical boiler, Therm. Sci. 17 (5) (2013) 1337–1342.
[4] R. Dhanuskodi, R. Kaliappan, S. Suresh, N. Anantharaman, A. Arunagiri, J. Krishnaiah, Artificial Neural Networks model for predicting wall temperature of supercritical boilers, App. Therm. Eng. 90 (2015) 749–753.
[5] Z. Zhang, Y. Yan, L. Zhang, Y. Chen, J. Ran, G. Pu, C. Qin, Theoretical study on CO_2 absorption from biogas by membrane contactors: effect of operating parameters, Ind. Eng. Chem. Res. 53 (36) (2014) 14075–14083.
[6] Y. Yan, Z. Zhang, L. Zhang, X. Wang, K. Liu, Z. Yang, Investigation of autothermal reforming of methane for hydrogen production in a spiral multi-cylinder micro-reactor used for mobile fuel cell, Int. J. Hydrogen Energy 40 (4) (2015) 1886–1893.
[7] X. Cheng, T. Schulenberg, Heat Transfer at Supercritical Pressures: Literature Review and Application to an HPLWR, FZKA, 2001.
[8] T. Yamashita, H. Mori, S. Yoshida, M. Ohno, Heat transfer and pressure drop of a supercritical pressure fluid flowing in a tube of small diameter, Memoirs Faculty Eng. 63 (4) (2003) 227–244.
[9] W. Hall, Heat transfer near the critical point, Adv. Heat Transf. 7 (1971) 1–86.
[10] B. Petukhov, A. Polyakof, V. Kuleshov, Y.L. Sheckter, Turbulent flow and heat transfer in horizontal tubes with substantial influence of thermo-gravitational forces, in: Proc. of Fifth Int. Heat Transfer Conference, 1974, pp. 3–7.
[11] M. Bazargan, D. Fraser, V. Chatoorgan, Effect of buoyancy on heat transfer in supercritical water flow in a horizontal round tube, J. Heat Trans-T ASME 127 (8) (2005) 897.
[12] J. Lee, P. Hejzlar, P. Saha, P. Stahle, M. Kazimi, D. McEligot, Deteriorated turbulent heat transfer (DTHT) of gas up-flow in a circular tube: experimental data, Int. J. Heat Mass Transfer 51 (13) (2008) 3259–3266.
[13] J. Lee, P. Hejzlar, P. Saha, M. Kazimi, D. McEligot, Deteriorated turbulent heat transfer (DTHT) of gas up-flow in a circular tube: heat transfer correlations, Int. J. Heat Mass Transfer 51 (21) (2008) 5318–5326.
[14] B.S. Shiralkar, P. Griffith, Deterioration in heat transfer to fluids at supercritical pressure and high heat fluxes, J. Heat Trans-T ASME 91 (1) (1969) 27–36.
[15] B. Shiralkar, P. Griffith, The effect of swirl, inlet conditions, flow direction, and tube diameter on the heat transfer to fluids at supercritical pressure, J. Heat Trans-T ASME 92 (3) (1970) 465–471.
[16] D. McEligot, C. Coon, H. Perkins, Relaminarization in tubes, Int. J. Heat Mass Transfer 13 (2) (1970) 431–433.
[17] D.M. McEligot, J.D. Jackson, "Deterioration" criteria for convective heat transfer in gas flow through non-circular ducts, Nucl. Eng. Des. 232 (3) (2004) 327–333.
[18] S. Liao, T. Zhao, An experimental investigation of convection heat transfer to supercritical carbon dioxide in miniature tubes, Int. J. Heat Mass Transfer 45 (25) (2002) 5025–5034.
[19] S.M. Liao, T.S. Zhao, Measurements of heat transfer coefficients from supercritical carbon dioxide flowing in horizontal mini/micro channels, J. Heat Trans-T ASME 124 (3) (2002) 413.
[20] P.-X. Jiang, R.-F. Shi, Y.-J. Xu, S. He, J. Jackson, Experimental investigation of flow resistance and convection heat transfer of CO_2 at supercritical pressures in a vertical porous tube, J. Supercrit. Fluid 38 (3) (2006) 339–346.
[21] P.-X. Jiang, Y. Zhang, Y.-J. Xu, R.-F. Shi, Experimental and numerical investigation of convection heat transfer of CO_2 at supercritical pressures in a vertical tube at low Reynolds numbers, Int. J. Therm. Sci. 47 (8) (2008) 998–1011.
[22] P.-X. Jiang, B. Liu, C.-R. Zhao, F. Luo, Convection heat transfer of supercritical pressure carbon dioxide in a vertical micro tube from transition to turbulent flow regime, Int. J. Heat Mass Transfer 56 (1) (2013) 741–749.
[23] J.R. Krieger, L.-D. Chen, Measurements of heat transfer to near-critical fluids, in: AIAA/ASME/SAE/ASEE Joint Propulsion Conference & Exhibit, 33 rd, Seattle, WA, 1997.
[24] D.L. Linne, M.L. Meyer, T. Edwards, D.A. Eitman, Evaluation of heat transfer and thermal stability of supercritical JP-7 fuel, AIAA Paper 3041 (1997) 1997.
[25] D.L. Linne, M.L. Meyer, D.C. Braun, D.J. Keller, Phenomena in Supercritical Fuels at High Heat Flux and Temperatures, 2000.
[26] B. Hitch, M. Karpuk, Experimental investigation of heat transfer and flow instabilities in supercritical fuels, AIAA Paper 3043 (1997).
[27] B. Hitch, M. Karpuk, Enhancement of heat transfer and elimination of flow oscillations in supercritical fuels, AIAA 3759 (1998).
[28] R.B. Duffey, I.L. Pioro, Experimental heat transfer of supercritical carbon dioxide flowing inside channels (survey), Nucl. Eng. Des. 235 (8) (2005) 913–924.
[29] I.L. Pioro, H.F. Khartabil, R.B. Duffey, Heat transfer to supercritical fluids flowing in channels—empirical correlations (survey), Nucl. Eng. Des. 230 (1–3) (2004) 69–91.
[30] I.L. Pioro, R.B. Duffey, T.J. Dumouchel, Hydraulic resistance of fluids flowing in channels at supercritical pressures (survey), Nucl. Eng. Des. 231 (2) (2004) 187–197.
[31] J.Y. Yoo, The turbulent flows of supercritical fluids with heat transfer, Annu. Rev. Fluid Mech. 45 (2013) 495–525.
[32] H. Deng, C. Zhang, G. Xu, Z. Tao, B. Zhang, G. Liu, Density measurements of endothermic hydrocarbon fuel at sub-and supercritical conditions, J. Chem. Eng. Data 56 (6) (2011) 2980–2986.
[33] H. Deng, K. Zhu, G. Xu, Z. Tao, C. Zhang, G. Liu, Isobaric specific heat capacity measurement for kerosene RP-3 in the near-critical and supercritical regions, J. Chem. Eng. Data 57 (2) (2011) 263–268.
[34] H. Deng, C. Zhang, G. Xu, Z. Tao, K. Zhu, Y. Wang, Visualization experiments of a specific fuel flow through quartz-glass tubes under both sub- and supercritical conditions, Chin. J. Aeronaut. 25 (3) (2012) 372–380.
[35] H. Deng, C. Zhang, G. Xu, B. Zhang, Z. Tao, K. Zhu, Viscosity measurements of endothermic hydrocarbon fuel from (298 to 788) K under supercritical pressure conditions, J. Chem. Eng. Data 57 (2) (2012) 358–365.
[36] X. Li, F. Zhong, X. Fan, X. Huai, J. Cai, Study of turbulent heat transfer of aviation kerosene flows in a curved pipe at supercritical pressure, App. Therm. Eng. 30 (13) (2010) 1845–1851.
[37] X. Li, X. Huai, J. Cai, F. Zhong, X. Fan, Z. Guo, Convective heat transfer characteristics of China RP-3 aviation kerosene at supercritical pressure, App. Therm. Eng. 31 (14–15) (2011) 2360–2366.
[38] H. Deng, K. Zhu, G. Xu, Z. Tao, J. Sun, Heat transfer characteristics of RP-3 kerosene at supercritical pressure in a vertical circular tube, J. Enhanc. Heat Transf. 19 (5) (2012).
[39] C. Zhang, G. Xu, L. Gao, Z. Tao, H. Deng, K. Zhu, Experimental investigation on heat transfer of a specific fuel (RP-3) flows through downward tubes at supercritical pressure, J. Supercrit. Fluid 72 (2012) 90–99.
[40] K. Zhu, G.-Q. Xu, Z. Tao, H.-W. Deng, Z.-H. Ran, C.-B. Zhang, Flow frictional resistance characteristics of kerosene RP-3 in horizontal circular tube at supercritical pressure, Exp. Therm. Fluid Sci. 44 (2013) 245–252.
[41] Z. Liu, H. Pan, S. Feng, Q. Bi, Dynamic behaviors of coking process during pyrolysis of China aviation kerosene RP-3, App. Therm. Eng. 91 (2015) 408–416.
[42] Z. Tao, Y. Fu, G. Xu, H. Deng, Z. Jia, Experimental study on influences of physical factors to supercritical RP-3 surface and liquid-space thermal oxidation coking, Energy Fuels 28 (9) (2014) 6098–6106.
[43] X. Pei, L. Hou, Secondary flow and oxidation coking deposition of aviation fuel, Fuel 167 (2016) 68–74.
[44] K. Xu, H. Meng, Numerical study of fluid flows and heat transfer of aviation kerosene with consideration of fuel pyrolysis and surface coking at supercritical pressures, Int. J. Heat Mass Transfer 95 (2016) 806–814.
[45] C. Zhang, H. Deng, G. Xu, W. Huang, K. Zhu, Enthalpy measurement and heat transfer investigation of RP-3 kerosene at supercritical pressure, J. Aerosp. Power 25 (2) (2010) 331–335.
[46] C. Lin, M. Ebadian, The effects of inlet turbulence on the development of fluid flow and heat transfer in a helically coiled pipe, Int. J. Heat Mass Transfer 42 (4) (1999) 739–751.